Spin polarization and dimer buckling at the Si(100)-2×1 surface

Emilio Artacho
Departamento de Física de la Materia Condensada, C-III, Universidad Autónoma de Madrid, 28049 Madrid, Spain

Félix Ynduráin*
Max-Planck-Institut für Festkörperforschung, Heisenbergstrasse 1, 7000 Stuttgart 80, Federal Republic of Germany

(Received 29 May 1990)

A spin-resolved nonparametrized calculation of the electronic structure of the Si(100)-2×1 surface is presented. The current symmetric and asymmetric dimer models are considered. An energy gain of about 0.5 eV per surface atom is gained by including spin correlations in the calculations. The electronic charge and spin densities in the vicinity of the surface are presented. The results of the calculations strongly suggest that the dimer buckling is much smaller than predicted by previous spin-independent calculations.

I. INTRODUCTION

The study of both the atomic and electronic structures of the Si(100)-2×1 surface has been the subject of intense experimental and theoretical research work since the low-energy-electron-diffraction measurements of Schlier and Farnsworth in 1959 (Ref. 1) revealed a 2×1 reconstruction pattern. Although the driving mechanism for the formation of the dimers is generally accepted, the asymmetry of the dimers has been questioned. From the experimental point of view, the results are to some extent contradictory. On one side scanning-tunneling-microscopy measurements indicate that the dimers are symmetric away from defects and impurities.[2,3] On the other side, grazing-incidence x-ray-diffraction measurements are interpreted in terms of asymmetric dimers.[4] Core-level shifts of the Si $2p$ levels are consistent with the symmetric dimer configuration.[5–7] Other experiments are compatible with both symmetric and asymmetric dimer configurations, as has already been discussed by the authors.[8]

There have been several spin-independent theoretical calculations of the electronic and geometrical structure of the Si(100)-2×1 surface.[9–18] Most of the calculations indicate that the asymmetric dimer model is the more stable one, although a recent calculation by Batra[18] finds an almost equal energy for the symmetric and asymmetric dimer configurations in agreement with previous calculations done by Pandey.[14] The surface band structure obtained in these calculations is in fair agreement with experimental data although a metallic surface is obtained even for the asymmetric[17] dimers and the calculated occupied surface band is about 0.5 eV above the experimental one.[11,17] It is remarkable that, in spite of the effort made, there is no general agreement on the geometrical structure of this surface.

In this work we present a nonparametrized calculation of the electronic structure of the Si(100)-2×1 surface taking into account possible spin arrangements other than uniform since, as it was pointed out, all previous calculations have neglected spin correlations within the dimers. However, cluster calculations[13] and a recent model calculation[8] reveal that spin correlations can be of paramount importance. The main aim of this work is not to establish the geometrical arrangement of the atoms at the surface but rather to understand the influence of considering explicitly the spin in the calculations both in the total energy and in the electronic charge distribution.

To calculate the electronic structure we use a recently developed nonparametrized linear-combination-of-atomic-orbitals method in which full spin-unrestricted Hartree-Fock calculations are performed in finite clusters of atoms in combination with infinite systems.

This work is organized as follows. In Sec. II we briefly discuss the method of calculation and some results for the electronic structure in the spin-restricted approximation are presented. In Sec. III we present the results of the spin-dependent calculation of the electronic structure at the surface. Surface densities of electronic states are presented. The passivation of the surface by As is also discussed. Finally in Sec. IV core-level-shift calculations are presented and the conclusions of our work are drawn.

II. METHOD OF CALCULATION: SPIN-INDEPENDENT RESULTS

The method of calculation is based on the linear-combination-of-atomic-orbitals (LCAO) approximation. To simplify the calculation we assume a minimal basis set at the silicon atoms to describe the valence electrons. In most of the calculations presented here the effect of core orbitals is simulated by appropriate atomic pseudopotentials,[19] although some all-electron calculation will be presented when analyzing core-level shifts. In order to obtain the Hamiltonian matrix elements between atomic orbitals for the different geometrical configurations considered in this work, we have performed self-consistent Hartree-Fock calculations in finite clusters of atoms.[20] In this way, when no spin correlation is allowed, the Hamiltonian matrix elements have the form

$$H_{ij}=H_{ij}^{\text{core}}+\sum_{k,l}P_{kl}[(ij|kl)-\tfrac{1}{2}(ik|jl)] , \quad (1)$$

where P_{kl} is the matrix element of the density operator between orbitals k and l and

$$P_{kl}=2\sum_{n}^{\text{occ}}C_k^nC_l^n . \quad (2)$$

H_{ij}^{core} stands for

$$H_{ij}^{\text{core}}=\left\langle i\left|-\tfrac{1}{2}\nabla^2+\sum_{\mathbf{R}}^{\text{ions}}\left[\frac{1}{|\mathbf{r}-\mathbf{R}|}+W(\mathbf{r}-\mathbf{R})\right]\right|j\right\rangle , \quad (3)$$

where W is the nonlocal pseudopotential.[19] The C_i^n are the coefficients of the atomic-orbitals wave functions in the expansion of the eigenvectors of the Hamiltonian. The double integrals $(ij|kl)$ have the form

$$(ij|kl)=\int\int\phi_i(\mathbf{r}_1)\phi_j(\mathbf{r}_1)|\mathbf{r}_1-\mathbf{r}_2|^{-1}\phi_k(\mathbf{r}_2)\phi_l(\mathbf{r}_2)d\mathbf{r}_1d\mathbf{r}_2 . \quad (4)$$

The calculation is done self-consistently in the cluster until the stable electronic configuration for a given distribution of atoms is obtained. The total electronic energy has the form

$$E_{\text{tot}}=\sum_{i,j}P_{ij}H_{ij}^{\text{core}}+\tfrac{1}{2}\sum_{ijkl}P_{ij}P_{kl}[(ij|kl)-\tfrac{1}{2}(ik|jl)] . \quad (5)$$

We have considered first a $Si_8H_{18}^*$ cluster to simulate the Si bulk. The cluster is such that all the silicon atoms are tetrahedrally coordinated, the outer ones being bonded to hydrogenlike saturators H*. When minimizing the total energy in the cluster we obtain an equilibrium nearest-neighbor distance of 2.33 Å. To obtain the bulk electronic structure we take the Hamiltonian matrix elements H_{ij} from the cluster calculations and transfer them to perform a standard crystal LCAO calculation. The crystal charge distribution when interactions between orbitals in up to second-neighbor atoms are considered is shown in Fig. 1. The result is in agreement with previous calculations, the double structure at the Si—Si bond being due to the limited basis set used in the calculation.

To study the electronic structure at the surface we consider a semi-infinite system. The electronic structure at the surface is calculated by using the transfer-matrix technique[21,22] to obtain the Green's-function matrix elements and from them the electronic charge is calculated. The Hamiltonian matrix elements near the surface are obtained from appropriate finite cluster calculations with the atomic structure of previously proposed dimer models. In particular we have considered the Chadi symmetric dimer model[10] and the Yin and Cohen asymmetric model.[11] To simulate these structures we have studied silicon clusters that include atoms up to the fourth layer to calculate the needed Hamiltonian matrix elements.

The charge distribution can be written as

$$\rho(\mathbf{r})=-(2/\pi)\sum_{i,j}\left[\int_{-\infty}^{E_F}\text{Im}\hat{G}_{ij}(E)dE\right]\phi_i(\mathbf{r})\phi_j(\mathbf{r}) , \quad (6)$$

where

$$\hat{G}_{ij}(E)\equiv\langle\hat{\phi}_i|(E-H)^{-1}|\hat{\phi}_j\rangle , \quad (7)$$

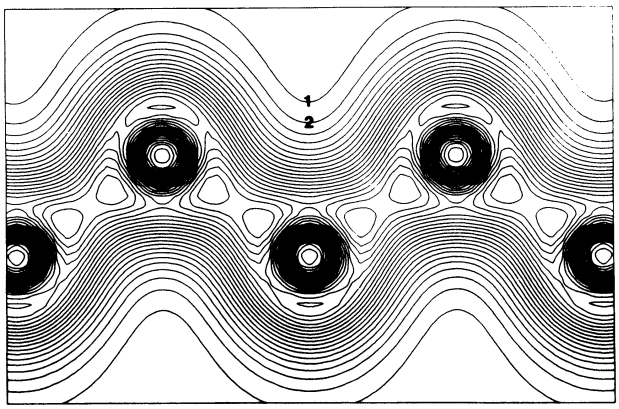

FIG. 1. Total valence electronic charge distribution at the silicon bulk in the second-nearest-neighbor approximation. The charge is plotted in the (011) plane passing through the atoms. The contour spacing is 1 and the units are electrons per bulk unit cell.

where $|\hat{\phi}_i\rangle$ stands for elements of the dual basis defined by

$$\langle\hat{\phi}_i|\phi_j\rangle=\delta_{ij} \quad (8)$$

and

$$\sum_i|\hat{\phi}_i\rangle\left\langle\phi_i|=\sum_i|\phi_i\right\rangle\langle\hat{\phi}_i|=1 , \quad (9)$$

and the $\hat{G}$'s satisfy the equation

$$\sum_i(E\langle\phi_j|\phi_i\rangle-\langle\phi_j|H|\phi_i\rangle)\langle\hat{\phi}_i|G(E)|\hat{\phi}_k\rangle=\delta_{jk} . \quad (10)$$

The charge distribution near the surface for the Chadi symmetric and the Yin and Cohen asymmetric dimer models is plotted in Figs. 2 and 3, respectively. The covalent bond formed between the surface atoms forming the dimer is clearly seen in the figures. The dangling-bond character pointing outwards is also clearly identified, as well as the partial ionic character of the bond formed in the asymmetric dimer model. There is a charge transfer between the atoms forming the dimers in the asymmetric case in such a way that the up atom has 0.055 extra charge essentially being transferred from the down one.

We cannot address our work to obtain equilibrium configurations since the surface relaxation penetrates into the bulk several layers. However, we have considered silicon clusters that include atoms up to the fourth layer and calculated the total energy. We obtain that the asymmetric geometry is more stable, the energy difference per dimer being 0.11 eV indicating a similar energy for the symmetric and asymmetric dimer models in agreement with previous local-density-approximation calculations. The lowering of the occupied surface-states band caused by the dimer asymmetry is responsible for the energy gain.

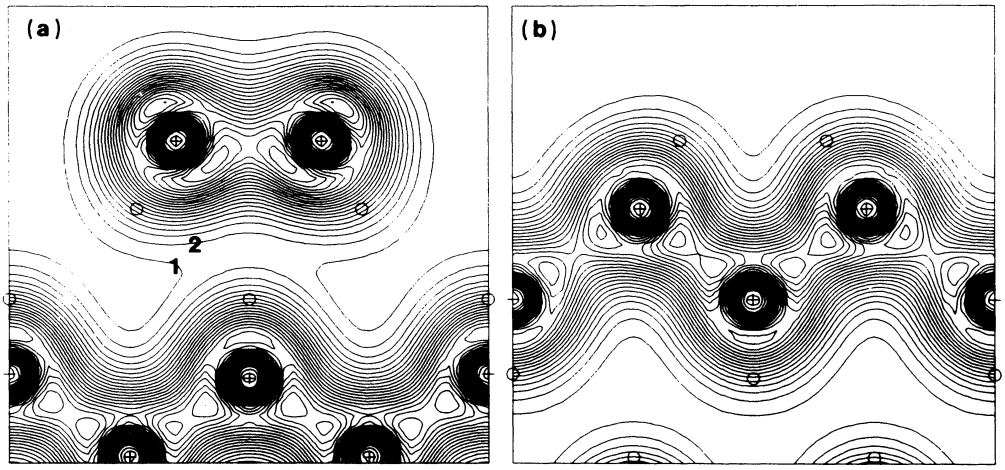

FIG. 2. Charge distribution near the surface for the symmetric Chadi model in the spin-restricted calculation plotted in (011) planes cutting the surface at right angles. Crosses and open circles represent silicon atoms contained in the plane and out of the plane, respectively. (a) Charge distribution at the (011) planes containing surface dimers. (b) Charge distribution at the (011) planes containing atoms of the second layer. The units are electrons per bulk unit cell and the contour spacing is 1.

III. SPIN-DEPENDENT CALCULATIONS

In this section we present the results we obtain for both the total energy and electronic distribution when releasing the spin-symmetry constraint. To this purpose we use the unrestricted Hartree-Fock method in which the spin-dependent Hamiltonian matrix elements have the form

$$H_{ij}^{\alpha,\beta}=H_{ij}^{\text{core}}+\sum_{k,l}[P_{kl}(ij|kl)-P_{kl}^{\alpha,\beta}(ik|jl)] , \tag{11}$$

with

$$P_{kl}^{\alpha,\beta}=\sum_{n}^{\text{occ}} C_k^{n\alpha,\beta}C_l^{n\alpha,\beta} \tag{12}$$

and

$$P_{kl}=P_{kl}^{\alpha}+P_{kl}^{\beta} , \tag{13}$$

where α and β stand for spin wave functions. The total electronic energy can be written in this case in the following form:

$$E_{\text{tot}}=\sum_{i,j}P_{ij}H_{ij}^{\text{core}} + \tfrac{1}{2}\sum_{ijkl}[P_{ij}P_{kl}-(P_{ik}^{\alpha}P_{jl}^{\alpha}+P_{ik}^{\beta}P_{jl}^{\beta})](ij|kl) . \tag{14}$$

The first interesting result of the calculations is that for both symmetric and asymmetric dimer models there is a

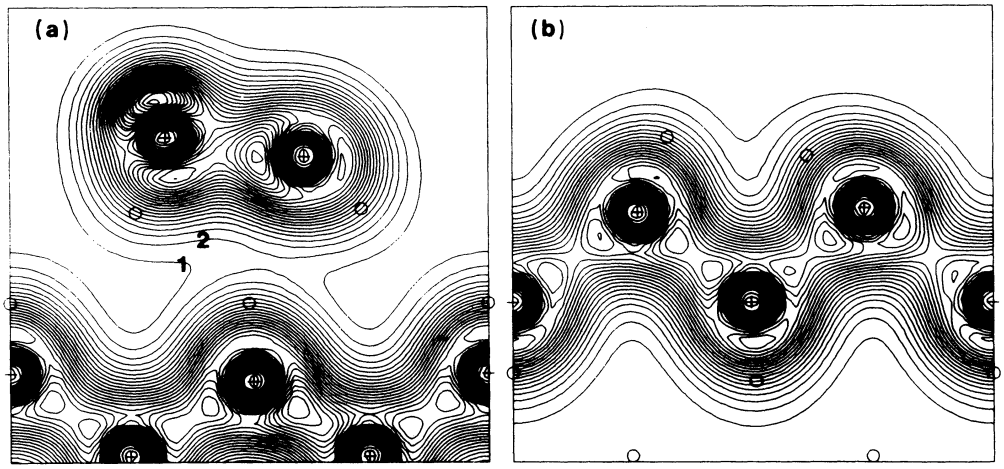

FIG. 3. Charge distribution near the surface for the asymmetric Yin and Cohen model in the spin-restricted calculation plotted in (011) planes cutting the surface at right angles. Crosses and open circles represent silicon atoms contained in the plane and out of the plane, respectively. (a) Charge distribution at the (011) planes containing surface dimers. (b) Charge distribution at the (011) planes containing atoms of the second layer. The units are electrons per bulk unit cell and the contour spacing is 1.

substantial gain of electronic energy in the cluster calculations by releasing the equal spin constraint. We obtain an energy gain of 2.08 and 1.05 eV per dimer for the symmetric and the asymmetric models, respectively. This result makes the symmetric dimer the more stable one, its energy being 0.92 eV lower than the asymmetric dimer. This large energy difference has to be considered with caution since no geometrical minimization when including spin has been performed. This result indicates the importance of including the spin in the calculation in both the symmetric and the asymmetric dimer models.

We have also calculated the charge and spin distribution in this case. The spin-dependent charge density is given by

$$\rho^{\alpha,\beta}(\mathbf{r})=-\frac{1}{\pi}\sum_{i,j}\left[\int_{-\infty}^{E_F}\mathrm{Im}\hat{G}_{ij}^{\alpha,\beta}(E)dE\right]\phi_i(\mathbf{r})\phi_j(\mathbf{r}) , \quad (15)$$

that can be used to compute

$$\rho(\mathbf{r})=\rho^{\alpha}(\mathbf{r})+\rho^{\beta}(\mathbf{r}) \quad (16)$$

and

$$\rho_{\mathrm{spin}}(\mathbf{r})=\rho^{\alpha}(\mathbf{r})-\rho^{\beta}(\mathbf{r}) , \quad (17)$$

i.e., total charge and spin density, respectively. The matrix elements $\hat{G}_{ij}^{\alpha,\beta}(E)$ are obtained by means of the relation

$$\sum_i (E\langle\phi_j|\phi_i\rangle-H_{ji}^{\alpha,\beta})\hat{G}_{ik}^{\alpha,\beta}(E)=\delta_{jk} . \quad (18)$$

In Fig. 4 we have plotted the spin-resolved charge densities for the symmetric dimer model. The asymmetric spin distribution is apparent in the figure. By adding and subtracting these charge distributions we obtain total charge and spin density, respectively.

In Fig. 5 we show the results for the Chadi symmetric dimer model. We observe that the total charge distribution is very similar to the restricted spin calculation (Fig. 2). The main difference in this case is the spin population of the two dangling bonds of the dimer, which in this case have opposite spin orientation. We also notice from the figure that the spin population is mostly localized at the surface layer decaying very rapidly towards the bulk.

The spin-resolved electronic structure for the Yin and Cohen asymmetric dimer model is presented in Fig. 6. In both cases the spin asymmetry is qualitatively the same: the local magnetic moments $\langle n_{i\uparrow}\rangle-\langle n_{i\downarrow}\rangle$ take the values -1.07 and 1.07 electrons for each atom of the symmetric dimer and -1.01 (1.14) electrons for the up (down) atom of the asymmetric dimer. These numbers

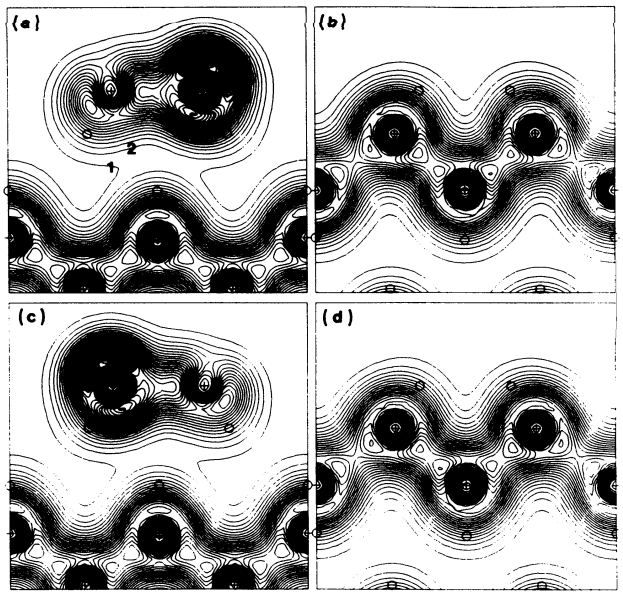

FIG. 4. Charge distribution per spin (multiplied by 2) near the surface for the symmetric Chadi model plotted in (011) planes cutting the surface at right angles. Crosses and open circles represent silicon atoms contained in the plane and out of the plane, respectively. (a) Charge distribution for up-spin electrons at the (011) planes containing surface dimers. (b) Charge distribution for up-spin electrons at the (011) planes containing atoms of the second layer. (c) Charge distribution for down-spin electrons at the (011) planes containing surface dimers. (d) Charge distribution for down-spin electrons at the (011) planes containing atoms of the second layer. The units are electrons per bulk unit cell and the contour spacing is 1.

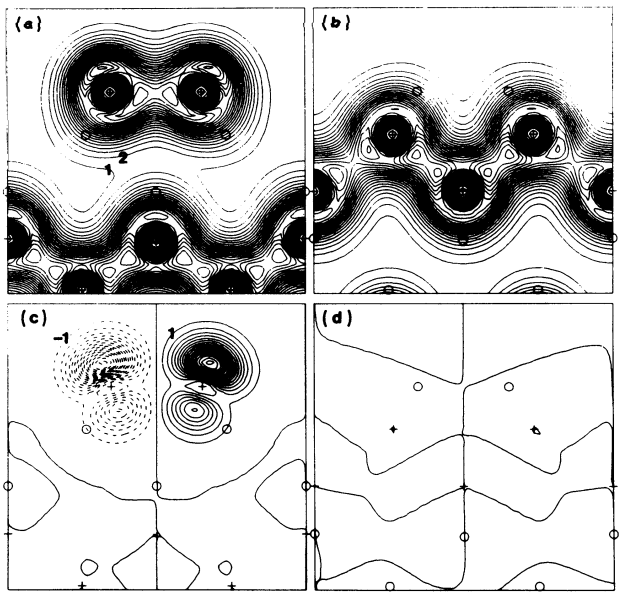

FIG. 5. Charge and spin distributions near the surface for the symmetric Chadi model in the spin-unrestricted calculation plotted in (011) planes cutting the surface at right angles. Crosses and open circles represent silicon atoms contained in the plane and out of the plane, respectively. (a) Total charge distribution at the (011) planes containing surface dimers. (b) Total charge distribution at the (011) planes containing atoms of the second layer. (c) Spin density at the (011) planes containing surface dimers. (d) Spin density at the (011) planes containing atoms of the second layer. The units are electrons per bulk unit cell and the contour spacing is 1.

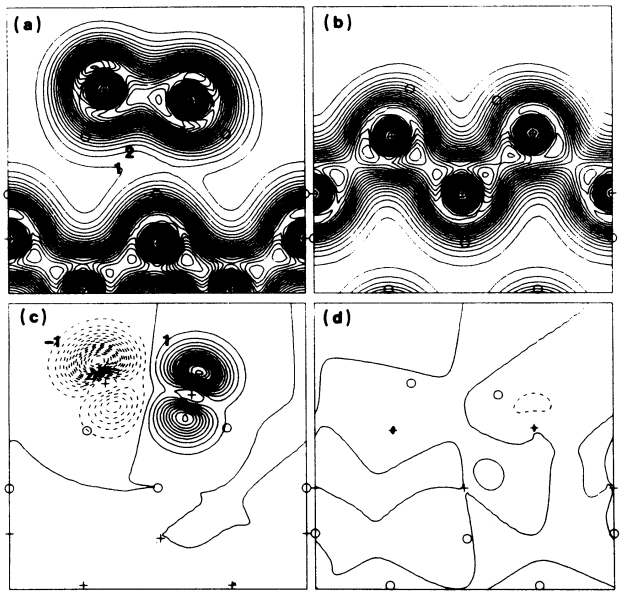

FIG. 6. Charge and spin distributions near the surface for the asymmetric Yin and Cohen model in the spin-unrestricted calculation plotted in (011) planes cutting the surface at right angles. Crosses and open circles represent silicon atoms contained in the plane and out of the plane, respectively. (a) Total charge distributions at the (011) planes containing surface dimers. (b) Total charge distribution at the (011) planes containing atoms of the second layer. (c) Spin density at the (011) planes containing surface dimers. (d) Spin density at the (011) planes containing atoms of the second layer. The units are electrons per bulk unit cell and the contour spacing is 1.

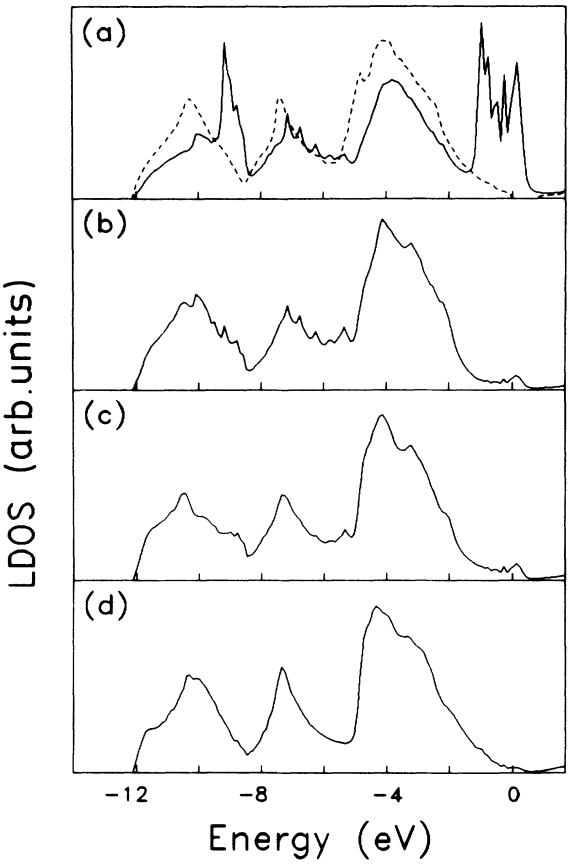

FIG. 7. Electronic densities of states near the surface for the symmetric dimer model for the restricted-spin calculation. (a), (b), (c), and (d) represent the densities of states corresponding to the first, second, third, and fourth layers, respectively. The energies are referred to the top of the bulk valence band. The dashed curve at the top panel represents the bulk density of states.

could be overestimated since no electronic correlation is included in the total-energy calculation.

For a better description of quasiparticle energies and proper comparison with spectroscopic experimental data, we have included in our calculations a self-energy diagonal term which takes into account the electronic correlation in second-order perturbation expansion in the electron-electron interaction.[23–25] This self-energy makes the valence bands narrower than the Hartree-Fock ones.

The results of the calculated densities of states at different layers near the surface for the symmetric dimer model are shown in Figs. 7 and 8 for the spin-restricted and -unrestricted calculations, respectively. We first observe that for the spin-restricted calculation the surface is metallic. The main effect of including explicitly the spin in the calculation is the shift of the occupied surface states towards lower energies making the surface semiconducting in agreement with experimental results. In addition, the surface-states band is located below the top of the valence band in agreement with experimental findings. This lowering is responsible for the energy gain when including explicitly the spin in the calculations.

We have also studied in the spin-resolved approximation the electronic structure of one monolayer of arsenic at the silicon surface for the Uhrberg *et al.* model.[26] Arsenic passivates its surface and it is expected that all the bonds are saturated. In Fig. 9 we present the spin-dependent results for an arsenic layer of atoms absorbed at the surface. The results present no spin asymmetry. The electronic charge pointing outwards at the As atoms corresponds to electrons in lone orbitals. As expected, there is a complete saturation of the silicon dangling bonds with no spin asymmetry in agreement with previous calculations.[26]

IV. CONCLUDING REMARKS

To complete our analysis we have calculated the $2p$ silicon levels at the surface for the two dimer models considered throughout this work, removing the pseudopotentials and performing all electron calculations.[8] The calculated chemical shifts with respect to bulk values together with the x-ray photoemission spectroscopy (XPS) experimental data[7] are shown in Fig. 10. We observe an excellent agreement for the symmetric dimer model and a nonexperimentally observed two-peak structure around 1 eV in the case of the asymmetric dimer, stressing again

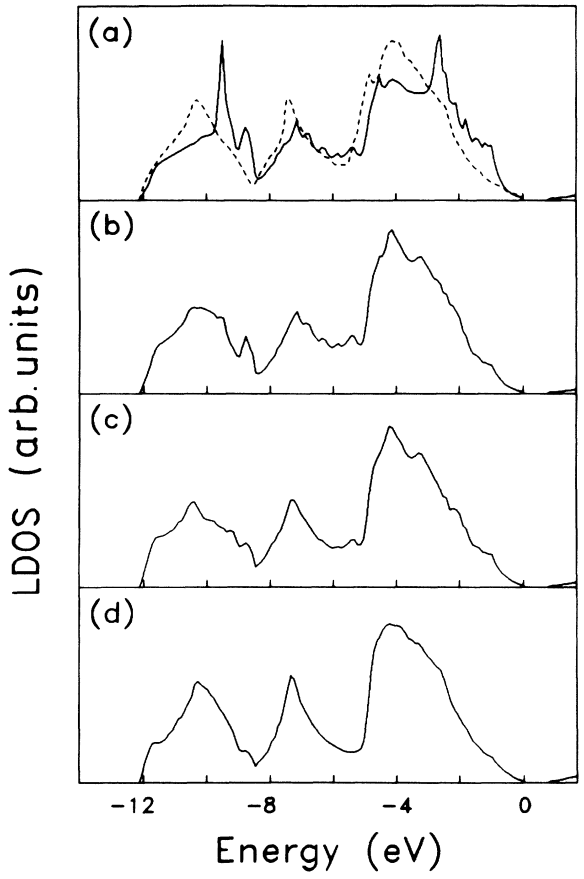

FIG. 8. Electronic densities of states near the surface for the symmetric dimer model for the unrestricted-spin calculation. (a), (b), (c), and (d) represent the densities of states corresponding to the first, second, third, and fourth layers, respectively. The dashed curve at the top panel represents the bulk density of states. The energies are referred to the top of the bulk valence band.

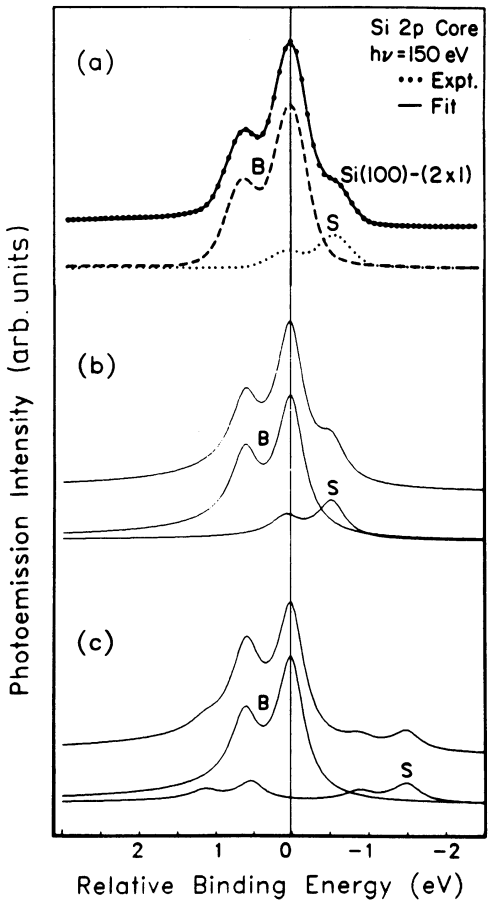

FIG. 10. Silicon $2p$ core level at the Si(100)-2×1 surface. In (a) the experiments of Ref. 7 are presented. (b) and (c) are the theoretical results obtained for Chadi symmetric and for Yin and Cohen asymmetric dimer models, respectively. The binding energies obtained for the $2p$ levels of surface and bulk silicon atoms, including a spin-orbit splitting of 0.61 eV (Ref. 7) are convoluted with properly weighted Doniach-Šunjić (Ref. 28) functions. S stands for surface and B for bulk signal with the sum of both shifted upwards for clarity.

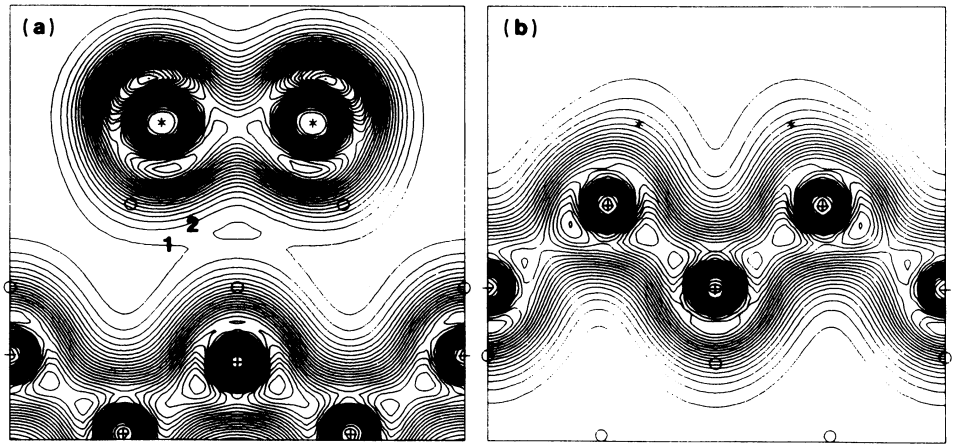

FIG. 9. Charge distribution near the surface for one As monolayer adsorbed at the Si(100) surface for the model of Ref. 26. The calculation is performed in the spin-unrestricted approximation. The charges are plotted in (011) planes cutting the surface at right angles. Stars stand for arsenic atoms. Crosses and open circles represent silicon atoms contained in the plane and out of the plane, respectively. (a) Total charge distribution at the (011) planes containing surface arsenic atoms. (b) Total charge distribution at the (011) planes containing atoms of the second layer. The units are electrons per bulk unit cell and the contour spacing is 1.

the favorable symmetric arrangement at the dimer in agreement with other core-level-shift calculations.[27]

From our calculations we can conclude the following.

(i) Inclusion of spin correlation when calculating the electronic structure and total energies for different atomic geometries at the Si(100)-2×1 surface seems essential to obtain reliable results.

(ii) We find that for all the current dimer models the spin arrangements within the dimers is antiferromagnetic for both the buckled and the nonbuckled models. Therefore it is essential to include the spin when calculating atomic and molecular adsorption at the surface.

(iii) We have analyzed other dimer models than those reported above. We have found for all the models considered that including spin correlation in the calculations makes the symmetric models more stable than the asymmetric ones. Hartree-Fock calculations tend to overestimate spin population. Nevertheless, in this case, the energy gain when releasing the spin symmetry is so large that inclusion of electron-electron correlation would not change our results substantially.

(iv) The electronic surface densities of states are in better agreement with experiments when including the spin explicitly in the calculation, the surface becoming semiconducting in agreement with experimental findings.

(v) Core-level-shift analysis indicates that the charge transfer associated with the buckled dimer models is not compatible with experimental findings.

(vi) All the above results indicate that dimers buckling (if any) at the surface are much smaller than previously predicted.

ACKNOWLEDGMENTS

This work was supported in part by Comisión Interministerial de Ciencia y Tecnología. One of us (F.Y.) would like to acknowledge support from the A. von Humboldt Foundation.

*Permanent address: Departamento de Física de la Materia Condensada, C-III, Universidad Autónoma de Madrid, 28049 Madrid, Spain.

[1]R. E. Schlier and H. E. Farnsworth, J. Chem. Phys. **30**, 917 (1959).

[2]R. M. Tromp, R. J. Hamers, and J. E. Demuth, Phys. Rev. Lett. **55**, 1303 (1985).

[3]R. J. Hamers, R. M. Tromp, and J. E. Demuth, Phys. Rev. B **24**, 5343 (1986); R. J. Hamers and U. K. Kohler, J. Vac. Sci. Technol. A **7**, 2854 (1989).

[4]N. Jedrecy, M. Sauvage-Simkin, R. Pinchaux, J. Massies, N. Greiser, and V. H. Etgens, Surf. Sci. **230**, 197 (1990).

[5]F. J. Himpsel, P. Heiman, T.-C. Chiang, and D. E. Eastman, Phys. Rev. Lett. **45**, 1112 (1980).

[6]D. H. Rich, A. Samsavar, T. Miller, H. F. Lin, T.-C. Chiang, J. E. Sundgren, and J. E. Green, Phys. Rev. Lett. **58**, 579 (1987); T.-C. Chiang, Mater. Res. Soc. Symp. Proc. **143**, 55 (1989).

[7]D. H. Rich, T. Miller, and T.-C. Chiang, Phys. Rev. B **37**, 3124 (1988).

[8]E. Artacho and F. Yndurain, Phys. Rev. Lett. **62**, 2491 (1989).

[9]J. A. Appelbaum and D. R. Hamann, Surf. Sci. **74**, 21 (1978).

[10]D. J. Chadi, Phys. Rev. Lett. **43**, 43 (1979), J. Vac. Sci. Technol. **16**, 1290 (1979).

[11]J. Ihm, M. L. Cohen, and D. J. Chadi, Phys. Rev. B **21**, 4592 (1980).

[12]M. T. Yin and M. L. Cohen, Phys. Rev. B **24**, 2303 (1981).

[13]A. Redondo and W. A. Goddard, J. Vac. Technol. **21**, 344 (1982).

[14]K. C. Pandey, in *Proceedings of the 17th International Conference on the Physics of Semiconductors,* edited by D. J. Chadi and W. A. Harrison (Springer, Berlin, 1984), p. 55.

[15]F. F. Abraham and I. P. Batra, Surf. Sci. **163**, L752 (1985).

[16]F. Bechstedt and D. Reichardt, Surf. Sci. **202**, 83 (1988).

[17]Z. Zhu, N. Shima, and M. Tsukada, Phys. Rev. B **40**, 11 868 (1989).

[18]I. P. Batra, Phys. Rev. B **41**, 5048 (1990).

[19]See, for instance, J. C. Barthelat, P. Durand, and A. Serafini, Mol. Phys. **33**, 159 (1977).

[20]P. Ordejón, E. Martínez, and F. Yndurain, Phys. Rev. B **40**, 12 416 (1989); E. Artacho and F. Yndurain (unpublished).

[21]L. M. Falicov and F. Yndurain, J. Phys. C **8**, 147 (1975); **8**, 1563 (1975).

[22]J. A. Vergés and F. Yndurain, Solid State Commun. **29**, 635 (1979).

[23]G. Díaz, E. Martínez, and F. Yndurain, Phys. Rev. Lett. **56**, 1731 (1986), and references therein.

[24]S. T. Pantelides, D. J. Mickish, and A. B. Kunz, Phys. Rev. B **10**, 2602 (1974).

[25]W. Borrmann and P. Fulde, Phys. Rev. B **35**, 9569 (1987).

[26]R. I. G. Uhrberg, R. D. Bringans, R. Z. Bachrach, and J. E. Northrup, Phys. Rev. Lett. **56**, 520 (1986).

[27]F. Bechstedt and D. Reichardt, Phys. Status Solidi B **157**, 567 (1990).

[28]S. Doniach and M. Šunjić, J. Phys. C **3**, 285 (1970).